EFFECTS OF INFILL WALLS ON BUILDING BEHAVIOUR UNDER SEISMIC LOADS

Lobzang Dorji

Lecturer, Department of Civil Engineering and Surveying, Jigme Namgyel Engineering College, Dewathang
Royal University of Bhutan.
Email: lobzangdorji21@gmail.com

Abstract: In the design of Reinforced Concrete (RC) building, infill walls are normally assumed as non-structural elements and they are accepted as vertical uniform loads on beams. Therefore, the RC buildings are designed as bare frame structures. However, in reality, infill walls are present in RC buildings, and the seismic performance of the buildings will be different with and without infill walls. In this study, 5 storey RC buildings with 2 bays and 5 bays in X-direction and Y-direction respectively are considered. The infill walls were replaced as equivalent diagonal struts and the non-linear static pushover analysis was performed to evaluate the effects of infill walls on the overall performance of the structures. The lateral strength capacity and performance point of the building were determined for the conventional (bare frame) method and with the presence of infill walls. The study reveals that the effects of infill walls under seismic loads in significant until elastic region in which the initial stiffness and strength of the structures increases, while lateral deformation capacity decreases. It is also observed that there are no significant changes in terms of ultimate lateral strength and roof displacement of the building as compared within presence of infill walls and bare frame.

Keywords: Pushover analysis, infill walls, capacity curve, Performance point.

I. INTRODUCTION

In developing countries, almost all the buildings are reinforced concrete (RC) frame buildings with masonry infill walls. The partition and exterior walls are usually constructed with the help of unreinforced masonry infill walls in buildings. Therefore, the universally accepted assumption in the design of frame structures is to neglect the structural role contributed by the infill panels as they are accepted as vertical uniform loads on beams and floors during seismic loads. However, the assumptions do not seem to agree with the reality when the building is subjected to seismic loads. The weight of the infill on the structure has been considered in the structural frame model but not the model in the design of a building. The model contains only beams, columns and slabs [5]. Therefore, this study aims to highlight the knowledge of the effects of infill walls on the RC frame structures, their sequences of failure through the formation of hinges and to evaluate the lateral strength capacity and performance point of the building under seismic loads.

II. PUSHOVER METHODOLOGY

The nonlinear static pushover analysis is one of the simplest options to determine the lateral strength capacity curve of the building, whereby, the evaluation of strength capacity within the post-elastic range is also made possible. In the pushover analysis, the lateral load pattern is distributed along with the height of

the building. The horizontal forces are constantly incremental with the displacement control at the top of the building until a certain level of deformation is achieved. The output of the pushover analysis is in the form of base shear and roof displacement as shown in Figures (1) and (2).
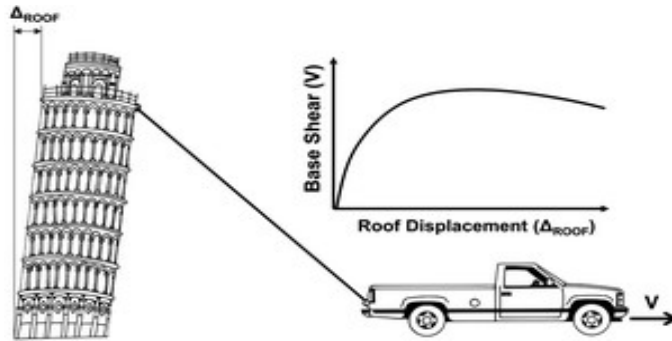
Fig. 1. Concept of pushover analysis [3]
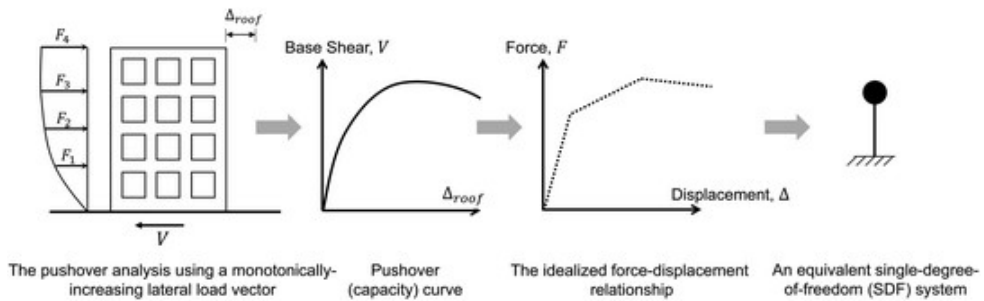
Fig. 2. Conversion of structural model in to SDF system [3]

2.1. Plastic Hinges

The plastic hinge symbolizes the post-yield behavior of the structures. The plastic deformation curve represents the force-displacement or moment-rotation curve, which gives the plastic deformation and the yield value. Figure (3) shows the moment rotation relationship for hinges to be used for pushover analysis. Point A and B represents the origin and yielding state respectively. Up to point B, there is no deformation occurs in the hinge. Beyond point B, there will be only plastic deformation exhibited by the hinges.
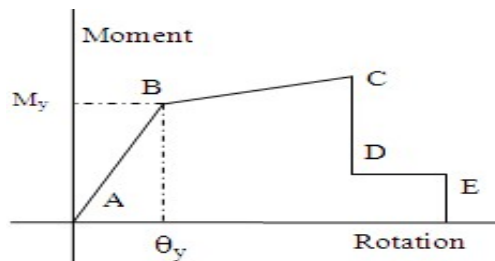
Fig. 3. Moment-Rotation relation for hinges [11]

In the pushover analysis, point C represents the ultimate capacity of the structures. The residual strength is represented by point D and the total failure of the structures is represented by Point E. The plastic hinge rotation capacities at points C, D and E can be derived from experimental or from the rational analysis using realistic material stress-strain relations. The plastic hinge rotation capacity at point B may obtain from the following equations (1-3).

$$\theta_y = \frac{M_y(L/2)}{4EI} \qquad \text{(For RC members) [6]} \qquad (1)$$

For steel element, FEMA-356 [8]

$$\theta_y = \frac{ZF_{ye}l_b}{6EI_b} \qquad \text{(For-beam)} \qquad (2)$$

$$\theta_y = \frac{ZF_{yc}l_c}{6EI_c}\left[1 - \frac{P}{P_{ye}}\right] \qquad \text{(For-column)} \qquad (3)$$

Where M_y is yield moment, L is the length of the member, E is Modulus of elasticity, θ_y is yield rotation, l_b is beam length, l_c is column length, and I_c and I_b are the moment of inertia of column and beam respectively. Z is plastic section modulus, F_{ye} is expected yield strength. P is the axial force in the member at the target displacement for nonlinear static analyses, and P_{ye} is the expected axial yield force of the member. In FEMA-356 [8] and ATC-40[1] recommended the plastic hinge rotation capacities of reinforced concrete beams and Columns at points **C**, **D** and **E**. In the study, these recommended values are used by SAP2000 program [12].

2.2. Capacity Spectrum Method

The capacity spectrum method (CSM) requires the construction of the capacity spectrum and demand curve to determine performance points. The pushover curve is converted to acceleration displacement response spectra (ADRS) format which is referred to as capacity spectrum curve (S_a versus S_d) [1]. These conversions are done by equations (4-7). The traditional demand spectrum curve estimated by reducing 5% damped is also converted to ADRS format by equation 9 and the representation is shown in Figure (4).

$$S_a = \frac{V/W}{\alpha_1} \qquad (4)$$

$$S_d = \frac{\Delta_{roof}}{PF_1\phi_{roof,1}} \qquad (5)$$

$$\alpha_1 = \frac{\left[\sum_{i=1}^{N}(w_i\phi_{i1})/g\right]^2}{\left[\sum_{i=1}^{N}w_i/g\right]\left[\sum_{i=1}^{N}(w_i\phi_{i1}^2)/g\right]} \qquad (6)$$

$$PF_1 = \left[\frac{\sum_{i=1}^{N}(w_i\phi_{i1})/g}{\sum_{i=1}^{N}(w_i\phi_{i1}^2)/g}\right] \qquad (7)$$

Where, PF1 is modal participation factor for first natural mode. α_1 is modal mass coefficient for first natural mode. w_i / g is mass assigned to level i. ϕ_{i1} is amplitude of mode 1 at level i. N is the upper most level of the structure. V is base shear. W is building dead weight plus likely lives. Δ_{roof} is roof displacement. T is a natural time period. S_a is spectral acceleration and S_d is spectral displacement.

$$S_d = \frac{S_a T^2}{4\pi^2} \tag{8}$$

$$T = 2\pi \sqrt{\frac{S_d}{S_a}} \tag{9}$$
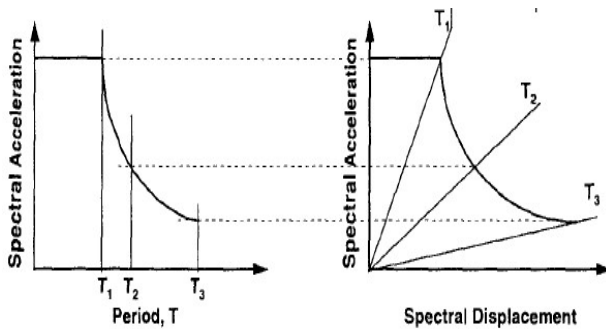
Fig. 4. Response spectra in traditional and ARDS format [1].

The capacity spectrum curve computed from pushover analysis is superimposed on the demand spectrum. The performance point is the intersection between these two curves as shown in Figure (5).
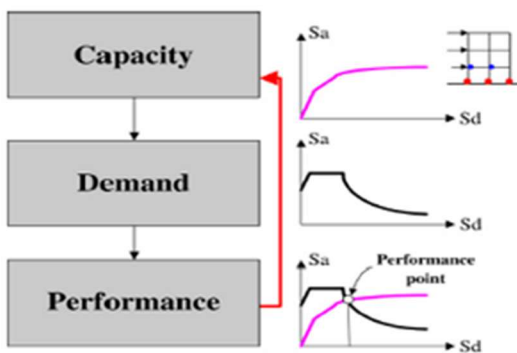
Fig. 5. Performance point of the building [12]

III. BUILDING DESCRIPTION

The typical five storey residential building having plan dimensions at all floor levels are 18.15 m x 8.45 m with the storey height of 3.2 m. The live loads have been assumed as 4 kN/m² as prescribed for residential buildings. The typical plan dimensions at all floor levels are 18.15 m x 8.45 m with a typical story height of 3.2 m as shown in the Figure (6).
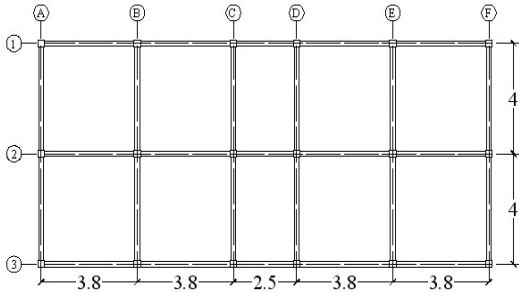
Fig. 6. Typical lay out plan of the building.
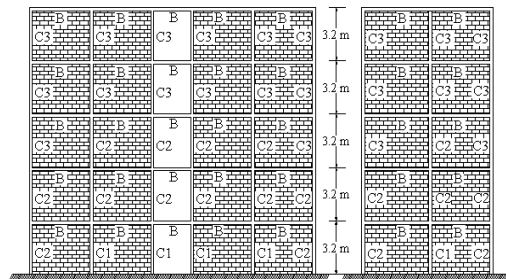
Fig. 7. Typical masonry infill RC frame.

The effects of infill walls of the selected building were done on two-dimensional models. The building plan is symmetry and the torsional amplifications are neglected. The typical planer multi-storey unreinforced infill walls RC frame with two bays in the weak direction (Frame along grid B) and five bays in strong direction (Frame along grid 2) is shown in Figure (7). Tables 1, 2, 3 and 4 present the material properties, typical dimensions, and reinforcement details of the selected building.

TABLE 1. Materials properties for different structural RC frame members

Characteristic compressive strength of concrete (MPa)	Ultimate tensile strength of main steel (MPa)	Ultimate tensile strength of distribution steel (MPa)
20	415	415

TABLE 2. Reinforcement details and the typical dimension of the member- Columns

Structural members	Longitudinal re-bars	Transverse re-bars	Column size (mm)
C1	8#25ø	8 ø@150c/c	350x350
C2	8#22ø	8 ø@150c/c	350x350
C3	8#22ø	8 ø @150c/c	300x300

TABLE 3. Reinforcement details and typical dimension of the member- Beams

Structural members	Longitudinal re-bars	Transverse re-bars	Beam Size (mm)
B	2#16 ø , 2#18 ø Top 2#18 ø Bottom	8@150/c	400x250

TABLE 4. Materials properties and design parameters for masonry infill

Masonry com. strength (MPa) f'm	Masonry compressive strain	Coefficient of friction of frame infill surface μ	Thickness of masonry infill (mm)	Density (kN/m³)	Modulus of elasticity (MPa) 550 f'm
3	0.002	0.3	125	20	1650

IV. MODELING APPROACH

The finite element package SAP 2000 has chosen for the analysis. The structural element such as beams and columns were modeled as line elements having plastic hinges at the ends of the element. The hinges properties available in SAP 2000 as per FEMA 356 [8] and 273 [7] are adopted in the analysis.

4.1. MODELING OF INFILL WALLS

The infill walls were modeled as equivalent single diagonal struts. The width of the equivalent diagonal strut Z was obtained from FEMA 306 [9] given by equation 10.

$$Z = 0.175(\lambda h)^{-0.4} d_m \qquad (10)$$

$$\lambda = \left[\frac{E_m t \sin 2\theta}{4 E_c I_g h_m} \right]^{1/4} \qquad (11)$$

Where h and h_m is the height of the column and infill respectively. E_c and E_m are modulus of elasticity of frame and infill materials respectively. I_g is the moment of inertia of the column. d_m is the diagonal length of infill panel. l_m and t are the length and thickness of the infill as shown in Figure (8). The lateral force-deformation relation of the strut shown in Figure (9) was obtained using the relation given in literature [10] base on several potential failure modes of infill masonry walls.
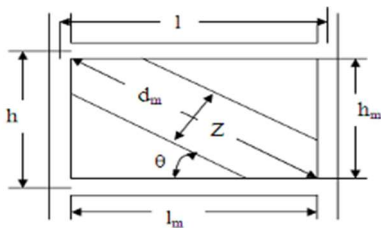
Fig. 8. Idealization of infill as diagonal strut [10]   **Fig. 9.** Strength develops in infill wall [10]
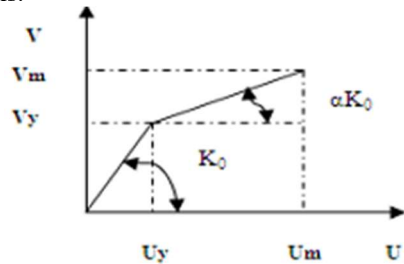
The failure due to sliding shear is the governing failure mode and the Mohr Coulomb failure criterion was applied to assess the maximum horizontal shear force given by equations 12.

$$V_f = \tau_0 t l_m + \mu N \qquad (12)$$

Where τ_0 is the cohesive capacity of the mortar bed, μ is the sliding friction coefficient along the bed joint and N is the vertical load on the infill wall. From Figure 7 maximum horizontal shear force V_f can be estimated from equation (13) and the vertical component of the diagonal compression force is given by $R_c \sin \theta$. From equations 12 and 13 V_f were calculated from equation 14.

$$V_f = R_c \cos \theta \qquad (13)$$

$$V_f = \frac{\tau_0 t l_m}{(1 - \mu \tan \theta)} = V_m \qquad (14)$$

The maximum displacement at maximum lateral force is estimated by equation 15 from literature [12].

$$U_m = \frac{\varepsilon'_m d_m}{\cos\theta} \qquad (15)$$

Where, $\varepsilon'_{æn}$ is the masonry compression strain at the maximum compression strain, the initial stiffness K_0 can be obtained from equation 16.

$$K_0 = 2(V_m / U_m) \qquad (16)$$

The lateral yield force V_y and displacement U_y were determined by equations 17 and 18 respectively.

$$V_y = \frac{V_m - \alpha K_0 U_m}{1-\alpha} \qquad (17)$$

$$U_y = \frac{V_y}{K_0} \qquad (18)$$

The value α is assumed to be equal to 0.2 from the literature [10]. The diagonal strut however only needs a hinge that represents the axial load. According to Al Chaar 2002 [2], the hinges to be at the mid-span of the members to represent the nonlinear behavior of the infill wall.

V. PUSHOVER ANALYSIS

The two-dimensional RC frame is pushed with monotonically increasing lateral loads until the collapse mechanism is obtained on the base shear and roof displacement plot. The pushover curve represents the inelastic limit as well as the lateral load-carrying capacity of the structures under earthquake excitation. Figure 10 shows an idealized force versus deformation curve that is used throughout the Guidelines to specify acceptance criteria for deformation-controlled components and element actions for any of the four basic types of materials. Linear response is illustrated between point A (unloaded component) and an effective yield point B. The slope from B to C is typically a small percentage (0–10%) of the elastic slope and is included to represent phenomena such as strain hardening. C has an ordinate that represents the strength of the component, and an abscissa value equal to the deformation at which significant strength degradation begins (line CD). Beyond point D, the component responds with substantially reduced strength to point E. At deformations greater than point E, the component strength is essentially zero according to FENA-273 [7]. Where, IO, LS and CP represent immediate occupancy, life safety and collapse prevention respectively.
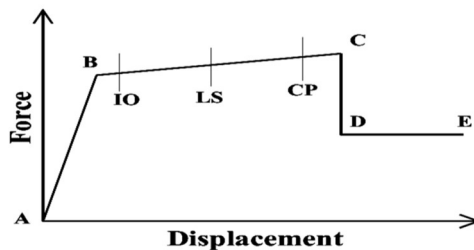
Fig. 10. Load–deformation curve [5].

VI. RESULT AND DISCUSSION

6.1. NOTATION

The lateral capacity of the building is presented by the capacity curve plotted between the normalized base shear versus roof displacement. Due to the constrained space available to be described the response of the structures during the pushover analysis, the general format citing a particular event can be written as *AA-AA [A]*. The first two characters represent the damage type of building component. The next two characters represent the component name. The last digit indicates the location of the component in the structures. As an example, the flexural yielding of *C1* at the first floor will be represented as *FY-C1 [1]*.

6.2. CAPACITY CURVE AND HINGES FORMATION

Figure (11), (13), (15) and (17) illustrates the capacity curves that depict the sequence of yielding and failure of the element for the selected building. The capacity curves show they are initially linear but start to deviate from linearity as the structural component undergoes inelastic actions. When the structure is pushed enough into the inelastic region, the curve becomes linear again with a lesser slope until ultimate lateral strength is achieved. It can be observed from these curves that the lateral capacity of the building starts dropping down at the first point when the structural members such as the beam undergo flexural failure. The overall capacity falls down penetratingly when structural members especially columns at lower stories are collapsed. The plastic hinge formation for the model has been obtained for the different events as shown in Figures (12), (14), (16) and (18). The plastic hinge formation for the bare frame begins with beam ends and then to column base of lower stories as the model is pushed sufficient until a predetermined target displacement is achieved. In the case of infill frame, hinge formation initiates from equivalent diagonal strut which reveals the failure of brick walls and then to rest of the structural components. This selected building shows a weak-beam strong-column mechanism from the analysis results.
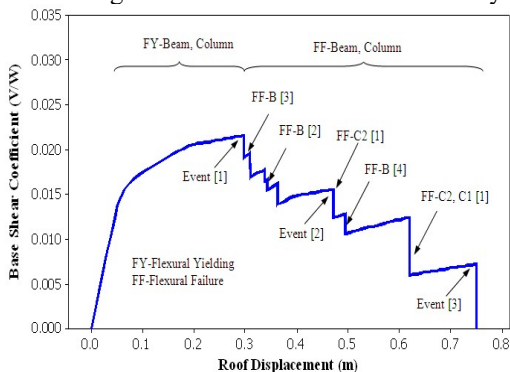
Fig. 11. Capacity curve of Bare Frame Y-Direction

Event (1)   Event (2)   Event (3)
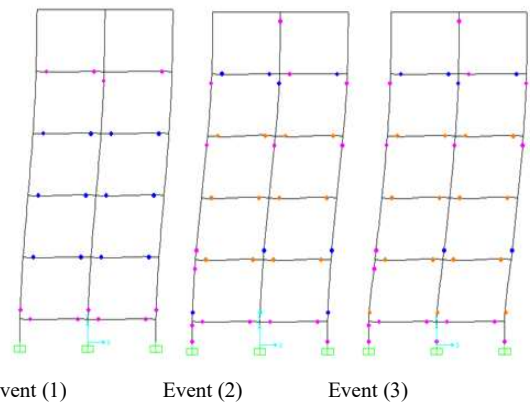
Fig. 12. Damage distribution and failure mechanism
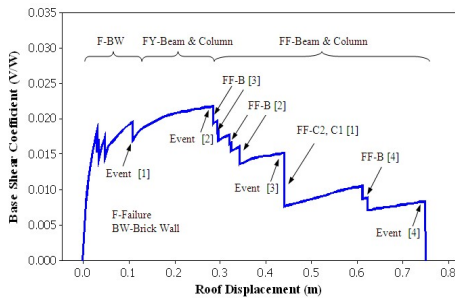
Fig. 13. Capacity curve of Infill Frame Y-Direction

Event (1) Event (2) Event (3) Event (4)
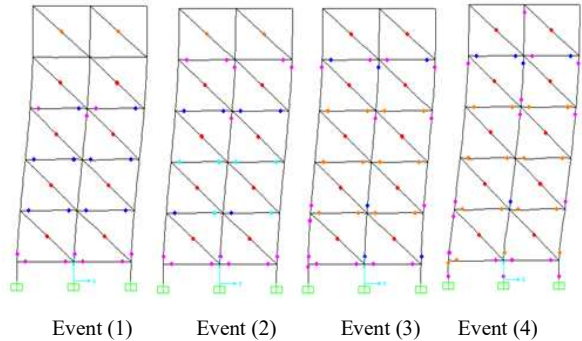
Fig. 14. Damage distribution and failure mechanism
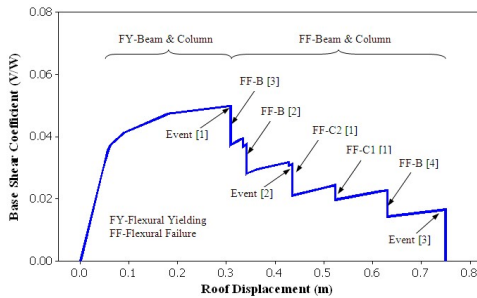
Fig. 15. Capacity curve of Bare Frame X-Direction

Event (1) Event (2) Event (3)
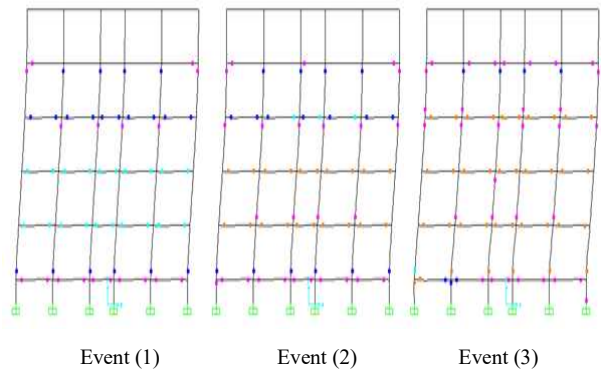
Fig. 16. Damage distribution and failure mechanism
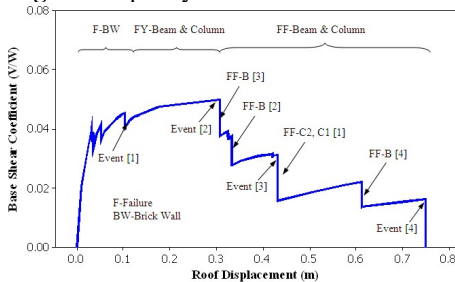
Fig. 17. Capacity curve of Infill Frame X-Direction

Event (1) Event (2) Event (3) Event (4)
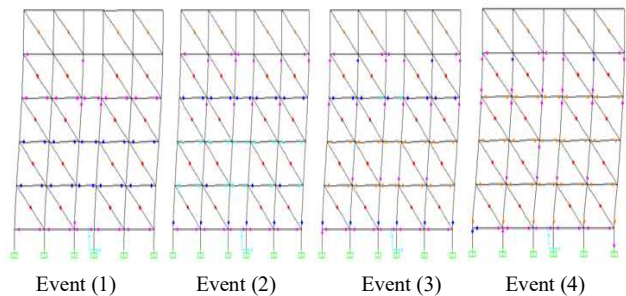
Fig. 18. Damage distribution and failure mechanism

6.3. EFFECTS OF INFILL WALLS ON THE CAPACITY CURVE

It is observed from Figure (19) that infill contributes to increasing the initial stiffness and strength while the deformation capacity of the structure reduces within the elastic region. The difference in ultimate strength and ultimate deformation capacity of the building is found negligible in presence of infill walls and bare frame. From the same Figure, it shows that for the frame along X-direction, the ultimate strength is very high as compared to the frame along Y-direction, although the difference in maximum roof displacement until collapsed is negligible. This is because the strength and stiffness increase when there is an increase in the number of bays.
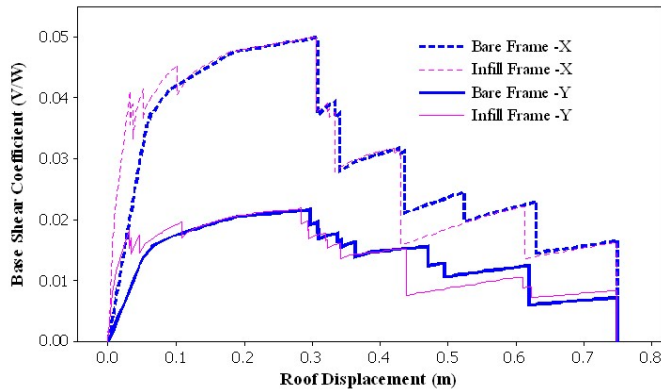
Fig. 19. Comparison of capacity curves in X and Y direction

6.4.   PERFORMANCE POINT OF THE BUILDING

The performance point which represents the global behavior of the building is shown in Figure (20) and (21) along with Y and X directions respectively. From Figure (20), the demand curve bisects the capacity curve within the point IO and CP. Similarly, from Figure (21), the demand intersects the capacity curve near point B, which is the effective yield point. It is obvious that the inelastic response and security margin exists in both directions along X and Y. The marginal safety against collapsed is high in the case of the frame along X-direction as there exists sufficient strength and displacement reserved as compared to the frame along Y-direction. The target displacement achieved from the analysis indicates that when the number of bays increases performance point tends to shift towards the linear region.
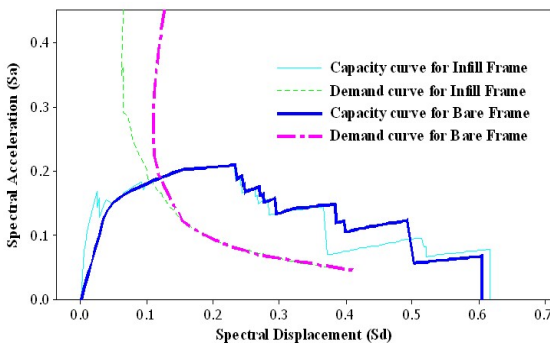
Fig. 20. Performance Point along Y-direction   **Fig. 21.** Performance Point along X-direction
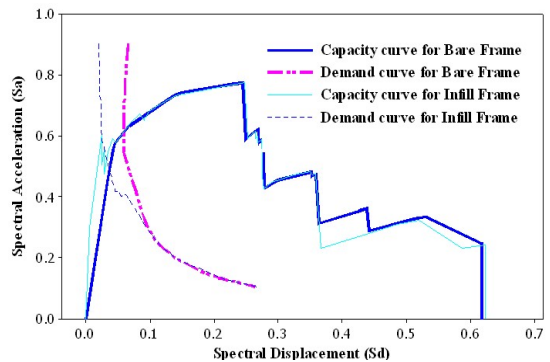
VII. CONCLUSIONS

The effects of infill walls on five-storey reinforced concrete buildings were studied using pushover analysis and the following conclusions are drawn:

- The effects of infill wall on seismic behavior of reinforced concrete frame building are significant until the elastic region in which the initial stiffness and strength increases while deformation capacity reduces.
- There is no significant increase and decrease in terms of ultimate strength and maximum roof displacement respectively in presence of infill masonry walls.

- The ultimate strength and initial stiffness increase drastically when the number of bay increases.
- The performance point tends to shift towards the linear region when the number of bays increases.
- The results of pushover analysis provide the physical behavior of the structures in terms of capacity, demand and plastic hinge formation.

The pushover analysis is comparatively easier to explore the inelastic action of the building structures through tracing the sequence of yielding and failure of each element of the structure.

REFERENCES

[1] Applied Technology Council, ATC 40, Seismic Evaluation and Retrofit of Concrete Buildings, California.

[2] Al Chaar (2002). Design of Fiber Reinforced Polymer Material for Seismic Rehabilitation of Infilled Concrete Structures. *US Army Corps of Engineers, Engineer Research and Development Centre, December 2002.*

[3] A.N Fawad (1017). Nonlinear Static Analysis procedures for seismic performance Evaluation of existing Building- Evaluation and Issues. *School of Engineering and Technology (SET). Asian Institute of Technology, Bangkok.*

[4] Ashraf and Stephen 1998. Practical Three Dimensional Nonlinear Static Pushover Analysis. *Published in Structure Magazine, winter 1998.*

[5] Cagatey. I. H (2005). Failure of Industrial Building during recent Earthquake in Turkey. Engineering Failure analysis 12 (2005) 497-507.

[6] Das and Murty (2004). Brick Masonry Infill in Seismic Design of RC Frame Buildings. *Indian Concrete Journal, August 2004.*

[7] FEMA-273, 1997. NEHRP Guidelines for the Seismic Rehabilitation of Buildings. Building Seismic Safety Council, Federal Emergency Management Agency, Washington.

[8] FEMA, NEHRP Guidelines for the seismic rehabilitation of buildings, FEMA-356, and NEHRP commentary on the guidelines for the seismic rehabilitation of buildings. Building Seismic Safety Council, Federal Emergency Management Agency, Washington.

[9] FEMA-306, Evaluation of Earthquake Damage Concrete and Masonry Wall Buildings. Building Seismic Safety Council, Federal Emergency Management Agency, Washington.

[10] Hossein and Toshimi (2004). Effect of infill Masonry Walls on the Seismic Response of Reinforced Concrete Buildings Subjected to the 2003 Bam Earthquake Strong Motion: A case study of Bam Telephone Centre. *Bulletin of the Earthquake Research Institute University of Tokyo. Vol. 79 (2004) PP. 133-156.*

[11] Phati Wet (2002). Seismic Evaluation of Beam-column Frame building with non-ductile reinforced Concrete details. *M. Eng. Thesis No. ST-02-12, Asian Institute of Technology.*

[12] SAP2000, Integrated Finite Elements and Design of Structures, Tutorial 2. *Computers and Structures Inc, Berkeley 1998, California USA.*